(Received 31 October 2023, Accepted 13 December 2023, Scheduled 26 December 2023)

Design of A Microstrip Filtering Antenna without Extra Circuits and Its Application in Orbital Angular Momentum (OAM) Filtering Antenna

Jia Liang[1,2], Dan Wang[1,*], Zisen Qi[1], Yun Gao[1], and Qingmei Wei[1]

[1] *Institute of Information and Navigation, Air Force Engineering University, Xi'an 710077, China*
[2] *Collaborative Innovation Center of Information Sensing and Understanding, Xi'an 710077, China*

ABSTRACT: In this paper, a microstrip filtering antenna is proposed with gain-filtering response. The antenna consists of an E-shaped radiator and a slotted U-shaped coupling structure. Three radiation nulls are obtained by the radiator, the U-shaped coupling structure, and the two slots. The filtering antenna has no extra circuits, which indicates that it is easy to design. A 4-element filtering OAM antenna array is also designed to validate its applicability in OAM antennas. Measured results show excellent performance of the array, which also make it a potential candidate for 5G wireless communication devices.

1. INTRODUCTION

In modern wireless communication devices, miniaturization and integration of radio wave components is always the popular trend. Antenna with filtering functions becomes a potential solution as it can help suppress the interference outside the operation bands.

In early designs of filtering antennas, filters are usually used as the feeding structure of the antennas. Antennas can be regarded as the last stage of filters. In this method, antennas and filters can be designed individually and then integrated together. Commonly, waveguide resonators or substrate-integrated-waveguides (SIW) can be used in filtering antenna designs [1–5]. For example, a dual-mode substrate integrated waveguide (SIW) cavity is used in [4] to generate two radiation nulls, and a quasi-elliptic filtering response of the radiation gain is obtained. A triple-mode cavity resonator is used in [5] to generate gain-filtering response, and a grid-slotted patch is used as the radiator. In recent years, a large number of antenna designs concentrate on the simplification of filters. New techniques such as split-ring resonators [6–9], open/shorted branches [10–17], and slots [11, 17–19] are used to obtain radiation nulls. For example, in [10], symmetric open branches are used to generate two radiation nulls outside the operation band, and the other radiation null comes from the radiating patch. The three radiation nulls contribute to a dual-band bandpass filtering performance of the radiation gain. In [12], two quarter wavelength branches are used as the feeding structure of a dielectric resonator antenna. The two branches offer two radiation nulls, which lead to a wideband bandpass filtering response of the radiation gain. Except for these designs, some other designs turn their attention to filtering antennas without filtering circuits [20, 21]. For example, in [20], electric and magnetic coupling is studied between radiators and parasitic structures, and two radiation nulls are designed with bandpass filtering performance. In [21], two square rings are utilized to generate two radiation nulls, and a wideband bandpass filtering response is obtained.

However, filtering antennas without extra circuits are still not easy to design as antennas get more compact under the trend of miniaturization. Besides, the application of filtering antennas in orbital angular momentum (OAM) antenna designs is seldom discussed. In view of this, a compact microstrip filtering antenna is designed without extra circuits. The origins of three radiation nulls are clearly stated and validated. The excellent performance of the filtering antenna can make it a design in 5G wireless communication devices. Further, four filtering antennas are used to form an OAM antenna array. The simulated and measured results can prove that the OAM array can also have radiation nulls of the filtering element, which indicate a new combination direction of OAM antenna and filtering antennas.

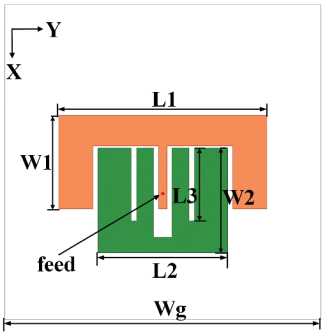

FIGURE 1. Geometry of the proposed microstrip filtering antenna. The main parameters are as follows (unit: mm): $L1 = 44.5$, $L2 = 32.1$, $L3 = 17.4$, $W1 = 19.3$, $W2 = 14.0$, $Wg = 80.0$.

* Corresponding author: Dan Wang (wangdan0709@126.com).

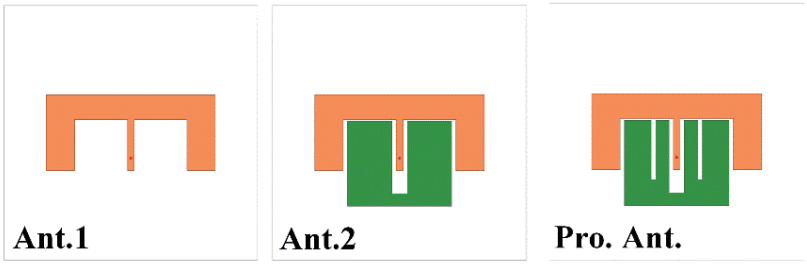

FIGURE 2. Evolution process of the proposed antenna.

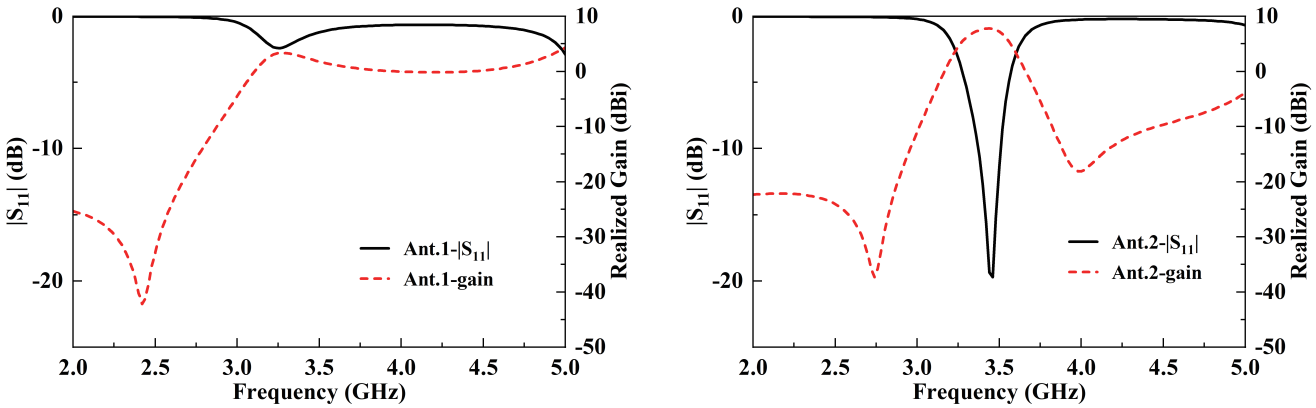

FIGURE 3. Simulated S-parameter and realized gain of Ant. 1 and Ant. 2.

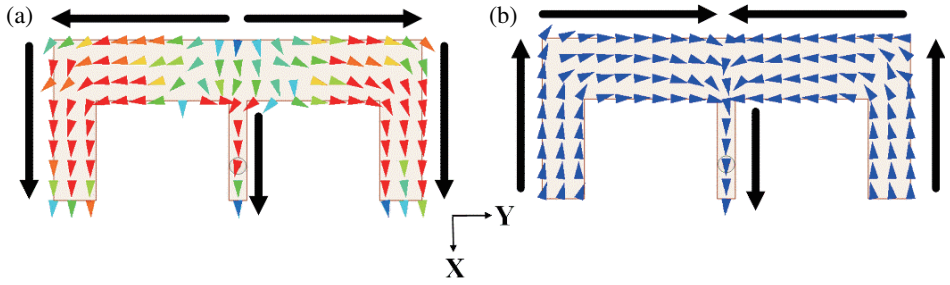

FIGURE 4. Current distributions on Ant. 1 at (a) 3.5 GHz and (b) 2.42 GHz.

2. DESIGN OF THE MICROSTRIP FILTERING ANTENNA

Figure 1 illustrates the geometry of the proposed antenna. The microstrip filtering antenna is printed on an F4B substrate with the permittivity of 2.65, loss tangent of 0.002, and thickness of 2 mm. The antenna exhibits a very simple structure with an E-shaped radiator and a slotted U-shaped coupling structure. The E-shaped radiator is fed by a coaxial cable through the hole of the substrate.

To elaborate the detailed working mechanism of the proposed antenna, an evolution process is given in Fig. 2. Ant. 1 is a conventional E-shaped radiator. Ant. 2 is a U-shaped coupling structure added to Ant. 1. The proposed antenna is two slots added to Ant. 2. The simulated $|S_{11}|$ and realized gain of Ant. 1 and Ant. 2 is plotted in Fig. 3. It can be seen clearly that Ant. 1 operates at about 3.25 GHz with a radiation null at 2.42 GHz. When the U-shaped coupling structure is added, Ant. 2 shows another radiation null at 4 GHz. To further study the origin of the radiation nulls, current distributions on Ant. 1 are shown in Fig. 4. The dominant currents at 3.25 GHz flow along the two arms of the radiator. As the currents along Y-axis are inverse, their radiation field cancel out in far field. Thus, the antenna shows a polarization direction along X-axis. Also, the currents at 2.42 GHz flow from one side end to the middle end, which shows longer path than the radiation mode at 3.25 GHz. Besides, the currents are all inverse along X-axis and Y-axis, which indicates cancellation of radiation field. As the currents at 2.42 GHz are very weak, the inherent radiation null is generated.

A parameter study is also developed to verify the radiation null of Ant. 1, as shown in Fig. 5. When the length of the radiator increases, the current path also increases, and the radiation null moves to lower band, which corresponds to the current distributions in Fig. 4.

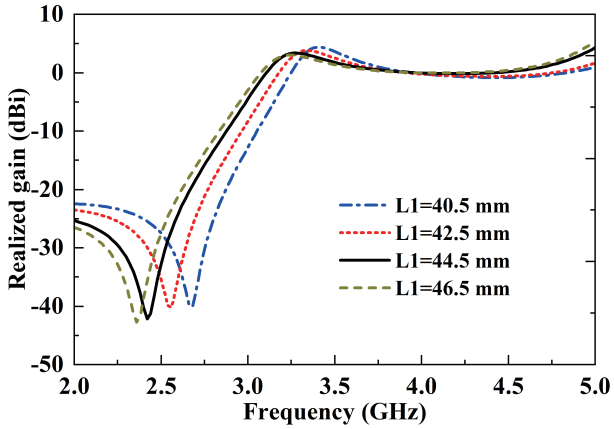

FIGURE 5. Radiation nulls varied with length of the radiator.

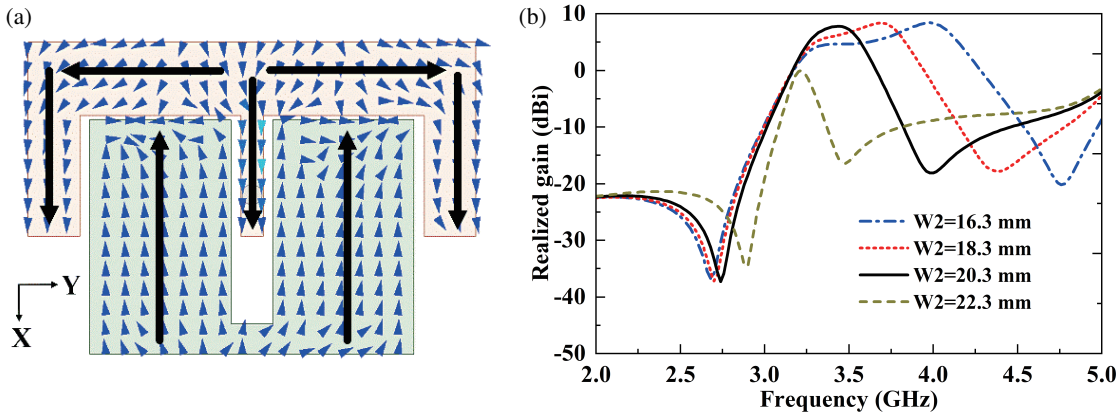

FIGURE 6. (a) Current distributions on Ant. 2 at 4.0 GHz. (b) Realized gain of Ant. 2 varied with $W2$.

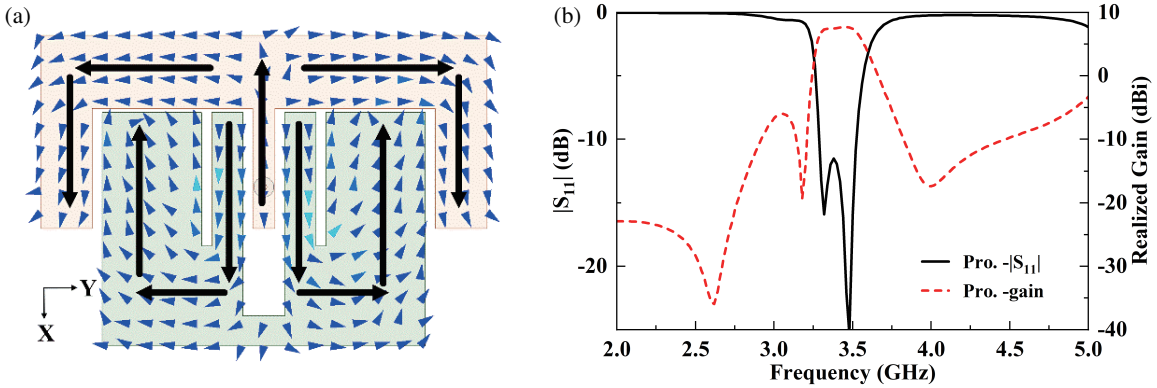

FIGURE 7. (a) current distribution at 3.18 GHz and (b) S-parameter, realized gain for the proposed antenna.

The radiation null introduced by the U-shaped coupling structure of Ant. 2 is located at 4.0 GHz. Its current distribution is also studied to figure out the origin of it, as illustrated in Fig. 6. With the symmetry of the antenna structure, currents on the U-shaped coupling structure are also symmetric about X-axis. Besides, currents on the E-shaped radiator are inverse, and the radiation field in far field is canceled out by the U-shaped coupling structure. Thus, the radiation null is obtained. It can be inferred that this null can be tuned by the parameters of the U-shaped coupling structure. For further study, the influence of length of the U-shaped coupling structure ($W2$) is carried out, as shown in Fig. 6(b). When $W2$ increases, the current length also gets longer, and radiation null at the upper band moves to low frequency band. Taking operation bandwidth of the microstrip antenna into account, 20.3 mm is chosen as a compromise value for $W2$.

As the filtering performance of the antenna at lower band is still not satisfied at lower band, another two slots are etched

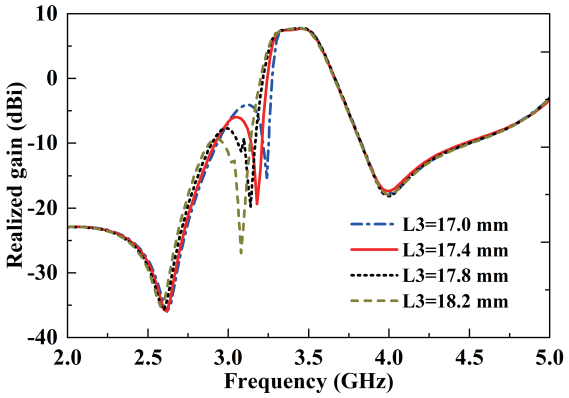

FIGURE 8. Realized gain of the proposed antenna varied with $L3$.

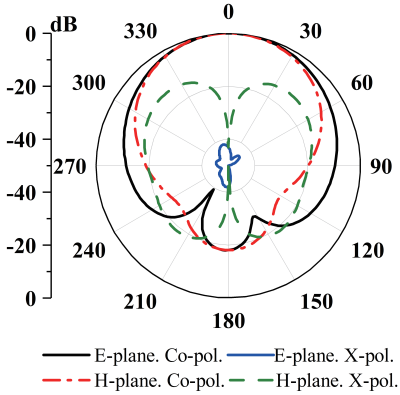

FIGURE 9. Normalized radiation pattern for the proposed antenna at 3.4 GHz.

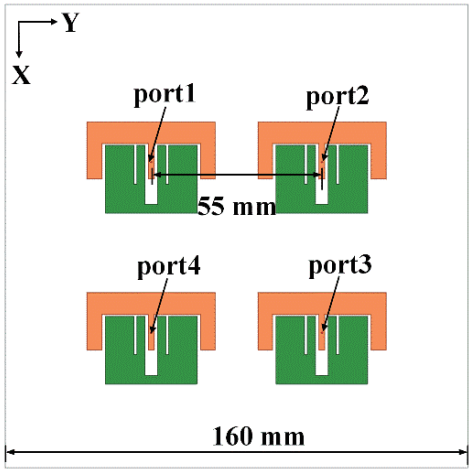

FIGURE 10. Configuration of the OAM antenna array.

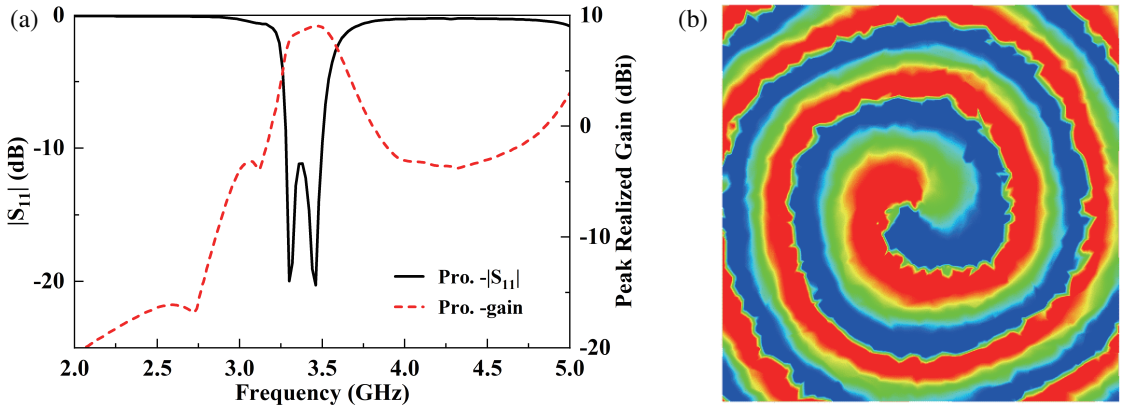

FIGURE 11. (a) Simulated S-parameter and realized gain and (b) helical phase distribution of the proposed OAM antenna array.

on the U-shaped coupling structure. The current distribution on the proposed antenna is shown in Fig. 7(a). It can be seen clearly that the currents on the coupling structure flow along the slots at 3.18 GHz. At the same time, all the currents are symmetric about X-axis, and the currents along Y-axis are inverse, which indicate that the radiation gain in far field is cancelled out, and a radiation null can be induced. The S-parameter and realized gain are plotted in Fig. 7(b). The third radiation null at 3.18 GHz is observed.

To validate the design concept, a parameter study is carried out, as shown in Fig. 8. The length of the slot $L3$ plays an important role in frequency of the third radiation null. When $L3$ increases, current path on the U-shaped coupling structure gets longer, and frequency of the third radiation null moves to

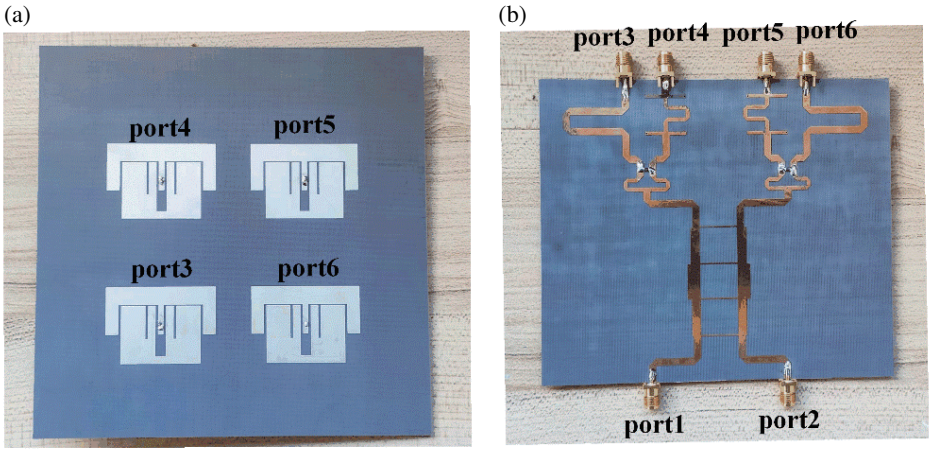

FIGURE 12. Prototype of the OAM antenna array and the feeding network. (a) Antenna array, (b) feeding network.

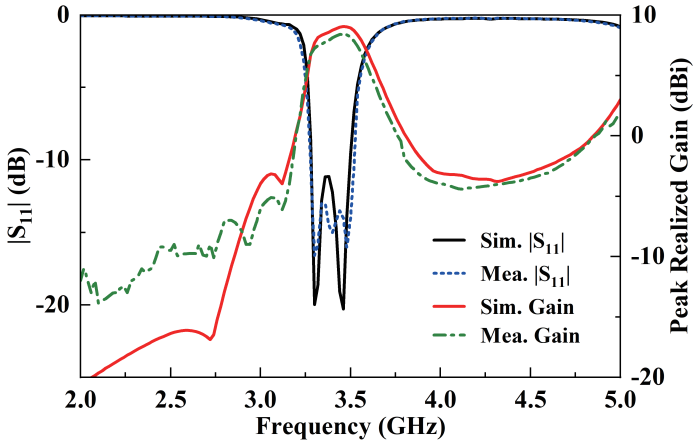

FIGURE 13. Simulated and measured S-parameters and realized gains of the OAM antenna array when port1 is fed.

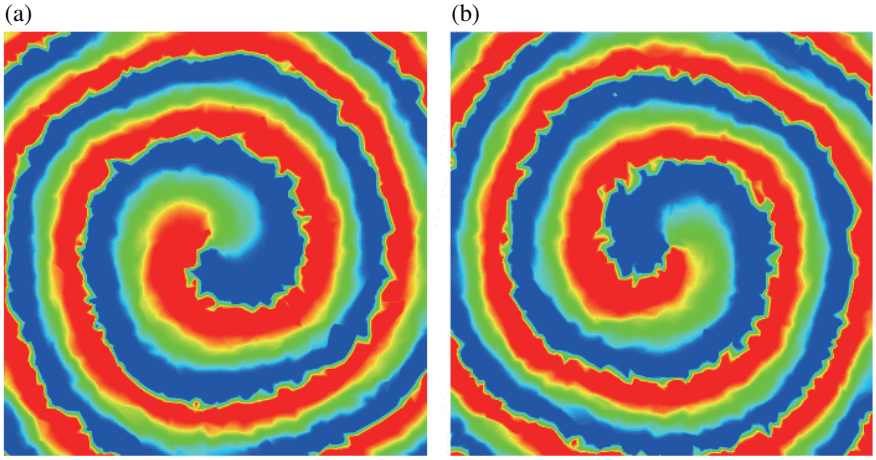

FIGURE 14. Measured helical phase distribution of the proposed OAM antenna array. (a) $+1$ mode, (b) -1 mode.

lower band. As a compromise, 17.4 mm is chosen for $L3$. Finally, the proposed filtering antenna shows an operation band of 3.28–3.52 GHz for $|S_{11}| < -10$ dB with three radiation nulls. The normalized radiation pattern for the proposed antenna at 3.4 GHz is also given in Fig. 9. Unidirectional radiation pattern is obtained with low cross-polarization, which indicates a good radiating performance.

3. OAM ANTENNA ARRAYS

A four-element antenna array is also designed to validate the applicability of the filtering antenna in OAM antenna designs, as shown in Fig. 10. The four ports are fed with sequential phase difference of 90 degrees to form the vertex phase of $+1$ mode. The simulated S-parameter and realized gain for the antenna array is illustrated in Fig. 11. The feeding network is shown in Fig. 12(b). The OAM antenna array has an operation bandwidth of 3.279–3.507 GHz for $|S_{11}| < -10$ dB. The peak realized gain is 6.68–9.04 dBi in the working band. Besides, the proposed antenna array shows a specific phase singularity, as well as a helical phase distribution of $+1$ mode.

4. RESULTS AND DISCUSSION

A prototype of the filtering OAM antenna array is fabricated and measured to validate the design concept, as shown in Fig. 12. A feeding network is also designed to form a dual-mode OAM antenna array. When port 1 is fed, the -1 mode vortex electromagnetic wave is obtained. On the other hand, the $+1$ mode can be obtained when port 2 is fed. The measured S-parameter and realized gains of the OAM antenna array are shown in Fig. 13. Good agreements can be observed between the measured results and simulated ones. The antenna array operates at 3.28–3.52 GHz for $|S_{11}| < -10$ dB. And the peak realized gain is 6.74–8.42 dBi in the working band. The difference between the measured gain and simulated results is mainly due to the loss in the feeding network. Fig. 14 shows the measured helical phase distribution of the proposed OAM antenna array. Both the modes show good vortex phase characteristics, which means that the proposed filtering antenna can be well designed for OAM antenna applications.

5. CONCLUSION

In this paper, a filtering microstrip antenna, as well as a filtering OAM antenna array is designed. The E-shaped antenna is proved to have an inherent radiation null owing to the symmetry of the antenna structure. By introducing a U-shaped coupling structure, a second radiation null is obtained at the upper band. Further, two slots are etched on the U-shaped coupling structure, and the third radiation null is obtained at lower band. Thus, the antenna has filtering response of the radiation gain. Further, a 4-element OAM antenna array is also designed to validate the filtering performance of OAM antennas. A feeding network is used to form two vortex modes. Simulated results show good agreements with the simulated ones. The designs of the filtering antenna and OAM antenna array indicate potential candidates in wireless communication devices.

ACKNOWLEDGEMENT

This work is supported by National Natural Science Foundation of China (Grant No. 62301599).

REFERENCES

[1] Wu, Y.-M., S.-W. Wong, H. Wong, and F.-C. Chen, "A design of bandwidth-enhanced cavity-backed slot filtenna using resonance windows," *IEEE Transactions on Antennas and Propagation*, Vol. 67, No. 3, 1926–1930, Mar. 2019.

[2] Chen, R.-S., S.-W. Wong, G.-L. Huang, Y. He, and L. Zhu, "Bandwidth-enhanced high-gain full-metal filtering slot antenna array using TE_{101} and TE_{301} cavity modes," *IEEE Antennas and Wireless Propagation Letters*, Vol. 20, No. 10, 1943–1947, Oct. 2021.

[3] Xie, H.-Y., B. Wu, Y.-L. Wang, C. Fan, J.-Z. Chen, and T. Su, "Wideband SIW filtering antenna with controllable radiation nulls using dual-mode cavities," *IEEE Antennas and Wireless Propagation Letters*, Vol. 20, No. 9, 1799–1803, Sep. 2021.

[4] Yang, M.-M., L. Zhang, Y. Zhang, H.-W. Yu, and Y.-C. Jiao, "Filtering antenna with quasi-elliptic response based on SIW H-plane horn," *IEEE Antennas and Wireless Propagation Letters*, Vol. 20, No. 7, 1302–1306, Jul. 2021.

[5] Xiang, K.-R., F.-C. Chen, and Q.-X. Chu, "High selectivity and high gain X-band waveguide filtering antenna based on triple-mode resonator," *IEEE Transactions on Antennas and Propagation*, Vol. 69, No. 10, 6953–6958, Oct. 2021.

[6] Qian, J.-F., F.-C. Chen, Y.-H. Ding, H.-T. Hu, and Q.-X. Chu, "A wide stopband filtering patch antenna and its application in MIMO system," *IEEE Transactions on Antennas and Propagation*, Vol. 67, No. 1, 654–658, Jan. 2019.

[7] Mao, C.-X., S. Gao, Y. Wang, Q. Luo, and Q.-X. Chu, "A shared-aperture dual-band dual-polarized filtering-antenna-array with improved frequency response," *IEEE Transactions on Antennas and Propagation*, Vol. 65, No. 4, 1836–1844, Apr. 2017.

[8] Mao, C.-X., S. Gao, Y. Wang, F. Qin, and Q.-X. Chu, "Compact highly integrated planar duplex antenna for wireless communications," *IEEE Transactions on Microwave Theory and Techniques*, Vol. 64, No. 7, 2006–2013, Jul. 2016.

[9] Rao, P. S., B. S. H. Prasad, J. Kavitha, and U. Jayaram, "A multi-slot UWB monopole antenna with dual band notch characteristics," *Progress In Electromagnetics Research C*, Vol. 138, 79–90, 2023.

[10] Li, Y., Z. Zhao, Z. Tang, and Y. Yin, "Differentially fed, dual-band dual-polarized filtering antenna with high selectivity for 5G sub-6 GHz base station applications," *IEEE Transactions on Antennas and Propagation*, Vol. 68, No. 4, 3231–3236, Apr. 2020.

[11] Li, Y., Z. Zhao, Z. Tang, and Y. Yin, "Differentially-fed, wide-band dual-polarized filtering antenna with novel feeding structure for 5G sub-6 GHz base station applications," *IEEE Access*, Vol. 7, 184 718–184 725, 2019.

[12] Hu, P. F., Y. M. Pan, X. Y. Zhang, and B. J. Hu, "A compact quasi-isotropic dielectric resonator antenna with filtering response," *IEEE Transactions on Antennas and Propagation*, Vol. 67, No. 2, 1294–1299, Feb. 2019.

[13] Xu, K., J. Shi, C. Zhang, and W. Liu, "A low-profile 1 x 2 filtering dipole array with small unit space and closely placed ground," *IEEE Antennas and Wireless Propagation Letters*, Vol. 18, No. 5, 946–950, May 2019.

[14] Wang, S., F. Fan, R. Gomez-Garcia, L. Yang, Y. Li, S.-W. Wong, and G. Zhang, "A planar absorptive-branch-loaded quasi-yagi antenna with filtering capability and flat gain," *IEEE Antennas and Wireless Propagation Letters*, Vol. 20, No. 9, 1626–1630, Sep. 2021.

[15] Wu, Q.-S., X. Zhang, and L. Zhu, "Co-design of a wideband circularly polarized filtering patch antenna with three minima in axial ratio response," *IEEE Transactions on Antennas and Propagation*, Vol. 66, No. 10, 5022–5030, Oct. 2018.

[16] Zhang, X. Y., Y. Zhang, Y.-M. Pan, and W. Duan, "Low-profile dual-band filtering patch antenna and its application to LTE MIMO system," *IEEE Transactions on Antennas and Propaga-*

tion, Vol. 65, No. 1, 103–113, Jan. 2017.

[17] Hu, H.-T., F.-C. Chen, and Q.-X. Chu, "Novel broadband filtering slotline antennas excited by multimode resonators," *IEEE Antennas and Wireless Propagation Letters*, Vol. 16, 489–492, 2017.

[18] Liu, X., K. W. Leung, and N. Yang, "Frequency reconfigurable filtering dielectric resonator antenna with harmonics suppression," *IEEE Transactions on Antennas and Propagation*, Vol. 69, No. 6, 3224–3233, Jun. 2021.

[19] Chen, X., Q. Zhuge, G. Han, R. Ma, J. Su, and W. Zhang, "A wideband harmonic suppression filtering antenna with multiple radiation nulls," *Progress In Electromagnetics Research Letters*, Vol. 112, 15–23, 2023.

[20] Qian, J.-F., F.-C. Chen, Q.-X. Chu, Q. Xue, and M. J. Lancaster, "A novel electric and magnetic gap-coupled broadband patch antenna with improved selectivity and its application in MIMO system," *IEEE Transactions on Antennas and Propagation*, Vol. 66, No. 10, 5625–5629, Oct. 2018.

[21] Ding, C. F., X. Y. Zhang, Y. Zhang, Y. M. Pan, and Q. Xue, "Compact broadband dual-polarized filtering dipole antenna with high selectivity for base-station applications," *IEEE Transactions on Antennas and Propagation*, Vol. 66, No. 11, 5747–5756, Nov. 2018.